

# A simple, internally consistent, and easily accessible means of calculating surface exposure ages or erosion rates from $^{10}\text{Be}$ and $^{26}\text{Al}$ measurements – DRAFT

Greg Balco <sup>a,\*</sup> John O. H. Stone <sup>a</sup>

<sup>a</sup> *Quaternary Research Center and Department of Earth and Space Sciences  
University of Washington, Mail Stop 351310, Seattle, WA 98195-1310 USA*

---

## Abstract

We codify previously published means of calculating exposure ages and erosion rates from  $^{10}\text{Be}$  and  $^{26}\text{Al}$  concentrations in rock surfaces, and present a single complete, straightforward, and internally consistent method that represents currently accepted practices. It is intended to enable geologists, geomorphologists, and paleoclimatologists, who wish to apply cosmogenic-nuclide exposure age or erosion rate measurements to their work, to: a) calculate exposure ages and erosion rates using a standard method; and b) compare previously published exposure ages or erosion rates on a common basis. The method is available online at <http://hess.ess.washington.edu/math>.

*Key words:* Cosmogenic nuclide geochronology, beryllium-10, aluminum-26, exposure-age dating, erosion rate measurements,

---

## 1 Introduction

### 1.1 Goals, capabilities, and limitations of the exposure-age calculator

In this paper we describe a method for calculating surface exposure ages and erosion rates from measurements of the cosmic-ray-produced radionuclides  $^{10}\text{Be}$  and  $^{26}\text{Al}$  in surface rock samples, which is available online via any commonly used web browser. This method essentially codifies previously published procedures for carrying out the various parts of the calculation. The importance of this contribution

---

\* Corresponding author. Tel. 206-221-2579

*Email addresses:* [balcs@u.washington.edu](mailto:balcs@u.washington.edu) (Greg Balco ),  
[stone@ess.washington.edu](mailto:stone@ess.washington.edu) (John O. H. Stone).

is not that we present significant improvements over previous calculation schemes, but that we have combined them in a simple and internally consistent fashion, and made the resulting method easily accessible via an online system, at the following URL:

*<http://hess.ess.washington.edu/math>*

This approach is intended to enable geologists, geomorphologists, and paleoclimatologists, who seek to use cosmogenic-nuclide exposure ages or erosion-rate measurements in their work, to easily calculate them using a standard method. This contribution is part of the CRONUS-Earth initiative, a multi-investigator project funded by the U.S. National Science Foundation whose goal is to improve the accuracy and usefulness of applications of cosmogenic-nuclide geochemistry to the Earth sciences.

We are motivated to develop an online exposure age and erosion rate calculator by the fact that the number of applications of cosmogenic-nuclide measurements, as well as the number of papers published on the subject, is growing rapidly. These studies are no longer being carried out exclusively by specialists in cosmogenic-nuclide geochemistry, but by Earth scientists who wish to apply cosmogenic-nuclide methods to broad research questions. These methods are still under development, so a variety of data-reduction procedures, reference nuclide production rates, and production rate scaling schemes exist in the literature. Many of these schemes are at least in part inconsistent with each other, and yield different results for the same measurements of nuclide concentrations. The effect of this has been that published exposure-age and erosion-rate data sets lack a common basis for comparison. For example, even without regard to the absolute accuracy of any of the exposure-age calculation methods relative to the true calendar year time scale, the variety of inconsistent calculation schemes makes it difficult even to compare the results of any two exposure-dating studies. This, in turn, is a serious obstacle for paleoclimate research or any other broader research task which relies on synthesizing the results of many studies. We seek to address this situation by providing a standard method that will enable anyone to easily calculate an exposure age or erosion rate, or compare previously published exposure ages or erosion rates in a consistent fashion.

The goal of the methods that we describe here is to provide an internally consistent result that reflects standard practices. At present, it is impossible to evaluate whether or not that they will always yield the 'right answer,' that is, for example, the correct calendar age for exposure-dating samples of all locations and ages. There are still many systematic uncertainties in the present understanding of nuclide production rates and scaling factors, and the methods we have chosen to use here may not prove to be the most accurate when more calibration data are available in future. We have chosen calculation methods, production rates, and production rate scaling schemes that are relatively straightforward to understand and use, are consistent with the calibration measurements that are available at present, and

are as consistent as possible with the majority of common usage in the existing literature. The purpose of the CRONUS-Earth project in general is to improve the accuracy of exposure-age and erosion rate calculations in two ways – first, by better understanding the physics of cosmogenic-nuclide production; second, by collecting a larger calibration data set to better evaluate the accuracy of production rate estimates and production rate scaling schemes. In future, therefore, we will have a better basis for choosing a reference production rate and scaling scheme, and more quantitatively evaluating its absolute accuracy.

### *1.2 Importance of comprehensive data reporting in cosmogenic-nuclide studies.*

One key goal of this work is to provide a common means of comparing exposure ages or erosion rates from different studies. This goal cannot succeed unless every investigator who publishes cosmogenic-nuclide exposure ages or erosion rates also reports all the information needed to recalculate them from the raw observations. In most cases this means: i) the location and elevation of the sample site; ii) the density, thickness and shielding geometry of the sample; iii) any independent information about the erosion rate of the sampled surface; and iv) the measured nuclide concentrations, corresponding analytical uncertainties, and the analytical standard against which the measurements were made. In other cases (e.g., complicated geometric corrections, unusual shielding histories), additional data are also needed.

If these data do not appear in full in a paper or associated data repository, then the exposure ages or erosion rates cannot be recalculated using a different calculation method, cannot be meaningfully compared with other data sets that use different calculation methods, and cannot be updated to reflect future improvements in the accuracy of production rates or scaling factors. Authors and reviewers of papers that use cosmogenic-nuclide measurements must do their best to ensure that all the information needed to duplicate the calculations actually appears in the paper.

### *1.3 Significant compromises and cautions*

Some aspects of calculating exposure ages or erosion rates involve simplifications or parameterizations for parts of the calculation that: i) are not well understood physically; ii) are well-understood, but difficult to calibrate by comparison to existing production rate measurements; or iii) must be simplified to make the calculation method computationally manageable. In some cases these compromises maintain the accuracy of the results for most applications, but reduce accuracy for certain unusual geometric situations or exposure histories. In other cases, we do not know the effect of these compromises on the accuracy of the results. Here we call atten-

tion to significant simplifications in our method and describe situations where they may lead to inaccurate results.

*Paleomagnetic field variation.* Physical principles clearly indicate that changes in the strength of the Earth's magnetic field should cause corresponding changes in cosmogenic-nuclide production rates at the Earth's surface. Several methods of accounting for past changes in magnetic field strength in calculating time-integrated surface production rates have been proposed in the literature (e.g., Nishiizumi et al., 1989; Dunai, 2001; Masarik et al., 2001; Desilets and Zreda, 2003; Pigati and Lifton, 2004); these give varying results. However, existing production rate calibration sites are poorly distributed in age to test the accuracy of these schemes. Thus, although we agree in principle that production rate scaling schemes should account for paleomagnetic variation, we have found that a time-invariant production rate scaling scheme fits the existing set of calibration measurements as well as any of the published time-varying schemes. In light of this observation, and the fact that the effect of magnetic field variations on production rates is still the subject of active research which will likely lead to significant future changes in published methods, we have assumed that nuclide production rates do not vary over time. In practice, this means that exposure ages computed with our method will be most accurate relative to true calendar ages for ages greater than ca. 10,000 yr B.P., that is, the age of most of the existing calibration sites. They may be less accurate relative to true calendar ages for middle Holocene ages, where paleomagnetic variations are expected to be most important. This may result in systematic uncertainties for Holocene samples of up to several percent in excess of the quoted uncertainty of the results of our method. Unfortunately, the existing calibration measurements are not sufficient to evaluate the importance of this effect. Gosse and Phillips (2001), Dunai (2001), Masarik et al. (2001), Desilets and Zreda (2003), and Pigati and Lifton (2004) discuss this issue in more detail.

*Geometric shielding of sample sites.* The geometric situation at and near a sample site affects nuclide production at the site in two ways: first, by shielding due to topography, which reduces the cosmic-ray flux that arrives at the sample site; second, by differences between the geometry of the sample site itself and the infinite flat surface usually assumed for purposes of production rate calculations, which are expected to reduce the production rate in the sample due to secondary particle leakage (e.g., Dunne et al., 1999; Masarik and Wieler, 2003; Lal and Chen, 2005). This means that both the surface production rate itself and the production rate - depth profile ought to differ from the ideal at heavily shielded, steeply dipping, or severely concave or convex sample locations. In keeping with common practice, we greatly simplify this part of the calculation by using only a single shielding factor that takes account of topographic obstructions and is computed using the typical angular distribution of cosmic radiation at the surface. We do not attempt to account for secondary particle leakage or for shielding and geometric effects on the depth dependence of the production rate. This means that our method will very likely have systematic inaccuracies for samples collected on steeply dipping sur-

faces (greater than approximately  $30^\circ$ ), in heavily shielded locations (e.g., at the foot of cliffs or in slot canyons), or in some other odd geometric situations. Users who seek extremely accurate results from samples in these pathological situations should consider this issue in more detail. Dunne et al. (1999), Masarik and Wieler (2003), and Lal and Chen (2005) discuss this in more detail.

*Cross-sections for nuclide production by fast muon interactions.* Our method of calculating erosion rates uses muon fluxes and production rates for fast muon interactions from Heisinger et al. (2002b), who rely on energy-dependent cross-sections for fast muon reactions that have only been measured at high muon energies. As most nuclide production by muons actually takes place at lower energies, it is difficult to evaluate the accuracy of this scheme in natural situations. It appears that production rates predicted by this scheme overestimate  $^{26}\text{Al}$  and  $^{10}\text{Be}$  concentrations measured in deep rock cores (Stone et al., 1998b, unpublished measurements by Stone), but the reason for this mismatch is unclear. Thus, it is possible that our method has systematic inaccuracies in the treatment of fast muon reactions, which in turn means that there may be systematic inaccuracies in calculating erosion rates when erosion rates are extremely high (greater than ca.  $0.5 \text{ cm} \cdot \text{yr}^{-1}$ ).

*Application to watershed-scale erosion rates.* Many erosion-rate studies seek to infer watershed-scale erosion rates from cosmogenic-nuclide concentrations in river sediment (e.g., von Blanckenburg, 2006; Bierman and Nichols, 2004). The method described here is designed for calculating surface erosion rates at a particular site and not for calculating basin-scale erosion rates. A strictly correct calculation of the basin-scale erosion rate requires a complete representation of the basin topography, which is not easily submitted to a central server. If supplied with the mean latitude and elevation of the watershed, however, the method described here will yield approximately correct results. For watersheds that do not span a large elevation range and otherwise satisfy the assumptions of the method, these results will most likely be within a few percent of the true spatially averaged erosion rate. In reality, this uncertainty is likely to be small relative to the uncertainty contributed by the many assumptions that are required to calculate a basin-scale erosion rate, in particular assumptions related to steady state and sediment mixing. However, users who seek very accurate basin-scale erosion rates, or are working in high-relief basins, should consider using a more physically correct calculation method. Bierman and Steig (1996), Brown et al. (1995), and Granger et al. (1996) describe basin-scale erosion rate measurements in more detail.

## 2 Description of the exposure-age calculator

### 2.1 System architecture

The exposure age and erosion rate calculator uses the MATLAB Web Server. MATLAB itself is a high-level programming language designed for mathematical computations. It is useful for this purpose because: i) it minimizes the need for low-level coding of numerical methods; ii) it is commonly used by geoscientists; and iii) MATLAB code is relatively easy to understand compared with lower-level programming languages.

The MATLAB Web Server is an extension to MATLAB that allows a web browser to submit data to a copy of MATLAB running on a central server, and receive the results of calculations, through standard web pages. We have chosen to use a central server, rather than distributing a standalone application that runs on a user's personal computer, because: i) the web-based input and output scheme is platform-independent; ii) the existence of only a single copy of the code minimizes maintenance effort and ensures that out-of-date versions of the software will not remain in circulation; and iii) the fact that all users are using the same copy of the code at a particular time makes it easy to trace exactly what method was used to calculate a particular set of results.

The software consists of two main components: a set of web pages that act as the user interface to the software, and a set of MATLAB functions ('m-files') that check input data, carry out calculations, and return results. Figure 1 gives an idea of the information flow. In this paper, we describe the major features of the calculation method, that is, the key equations, constants, and reference data. Appendix 1 contains detailed descriptions of all of the MATLAB functions .

### 2.2 Inputs

Table 1 shows the measurements and observations needed to calculate an exposure age or an erosion rate from  $^{10}\text{Be}$  or  $^{26}\text{Al}$  concentrations. Most are self-explanatory; two require further discussion.

First, in order to ensure the highest degree of consistency between exposure ages calculated using this system, one ought to define the required input data such that only direct measurements are used as inputs, and all derived quantities are produced internally by the calculator. We violate this rule by asking for a derived 'shielding correction' as input, rather than the actual measurements of the horizon geometry, strike and dip of the sampled surface, etc. We have chosen to do this because there is at present no standard method of recording the horizon and sample geometries,

and direct measurements are rare in the existing literature, so choosing one method of description would make it unnecessarily hard to recalculate previously published measurements. The difficulty is that the currently accepted method of computing this shielding correction (which we do make available to users via a separate input page) is physically deficient in some respects, and we expect that it will be improved in future. This means that if researchers report only the shielding correction computed with the present method, and not the actual sample and horizon geometry, it will be impossible to recalculate their results with improved methods in future. Thus, we strongly encourage researchers who publish cosmogenic-nuclide measurements to report all their direct measurements of the sample and horizon geometry, not just the shielding correction derived therefrom.

Second, we ask for nuclide concentrations ( $\text{atoms} \cdot \text{g}^{-1}$ ) as input rather than isotope ratios. This means that users must convert the isotope ratios provided by an AMS laboratory into nuclide concentrations. This part of the calculation cannot be done online because reducing isotope ratios to nuclide concentrations involves information and procedures specific to the laboratory where the chemical processing was done, most importantly the procedure for taking account of carrier and process blank concentrations. Thus, the user must convert isotope ratios to nuclide concentrations, and make appropriate blank corrections, offline. We do provide an outline of how to do this in the online documentation.

Furthermore, there exist different measurement standards for  $^{10}\text{Be}$  and  $^{26}\text{Al}$  that are in use at various AMS laboratories. Nuclide concentrations submitted to the calculator must be normalized to a single standard in order to be consistent with the production rate calibrations that we use. We have chosen to use the Nishiizumi  $^{10}\text{Be}$  and  $^{26}\text{Al}$  standards, which are described in Nishiizumi (2002) and Nishiizumi (2004). These are in use as the primary standards at several AMS laboratories, including the Center for Accelerator Mass Spectrometry at Lawrence Livermore National Laboratory (LLNL-CAMS). The user must make sure that measurements made at other AMS facilities are compatible with these standards. For example, the Purdue Rare Isotope Measurement Lab (PRIME Lab) has in the past instructed users to multiply  $^{10}\text{Be}$  isotope ratios reported by PRIME Lab by a factor of 1.14 to make them consistent with the Nishiizumi standards and thus with LLNL measurements. Similar adjustments may be required for data from other AMS facilities. Users who need more information about this should contact the AMS facility responsible for their measurements.

### 2.3 *Outputs*

The exposure age and erosion rate calculations return three things:

- (1) *Version information*. Numbers identifying the version of each component of

the software that was used in the calculation. Users should keep track of these version numbers as a record of exactly what calculation method was used.

- (2) *Results of the calculation.* Tables 2 and 3 describe these. Most are self-explanatory; the only aspect of the results that requires further discussion is the difference between internal and external uncertainties, which we discuss below in Section 2.9.
- (3) *Diagnostic information.* This information allows the user to verify that the rootfinding algorithm used in the erosion rate calculation converges properly. This is not relevant for most users and exists to facilitate debugging during the present review and testing of the system.

## 2.4 Constants

Most of the physical constants and parameters that are used in the calculation are either nuclide production rates, which are described in the next section, or are specific to particular parts of the calculation and are described in the function reference in Appendix 1. Three constants occur throughout the calculations and thus we document them here; these include the effective attenuation length for production by neutron spallation and the  $^{10}\text{Be}$  and  $^{26}\text{Al}$  decay constants.

We take the effective attenuation length for production by neutron spallation (denoted  $\Lambda_{sp}$  here and in most other work) to be  $160 \text{ g} \cdot \text{cm}^{-2}$ . Gosse and Phillips (2001) review measurements of  $\Lambda_{sp}$  in detail.

The absolute isotope ratios assigned to the Nishiizumi  $^{10}\text{Be}$  and  $^{26}\text{Al}$  measurement standards, to which we have normalized our calibration measurements, are dependent on particular choices of the decay constants. Thus, our choice of values for the decay constants is determined by our choice of measurement standards. These values are  $4.62 \times 10^{-7} \text{ yr}^{-1}$  and  $9.83 \times 10^{-7} \text{ yr}^{-1}$  for  $^{10}\text{Be}$  and  $^{26}\text{Al}$  respectively (Nishiizumi, 2002, 2004).

## 2.5 Production-rate scaling factors and reference production rates

Calculating cosmogenic-nuclide production rates at a particular location requires two things: first, a scaling scheme that describes the variation of the production rate with time, location, and elevation; and second, a reference production rate at a particular location, usually taken to be sea level and high latitude. This reference production rate is not measured directly, but is determined by: i) measuring either short-term nuclide production rates in artificial targets, or nuclide concentrations in surfaces of known exposure age, at a series of calibration sites; ii) using the scaling scheme to scale these measured local production rates to the reference location; and iii) averaging the resulting set of reference production rates to yield a best estimate

of the true value. Thus, given a particular set of calibration measurements normalized to a particular measurement standard, each scaling scheme yields one and only one reference production rate that can be used with that scaling scheme. The accuracy of the scaling scheme and associated reference production rate can then to some extent be evaluated by asking how well the production rates predicted for the calibration sites match the measured local production rates, usually by computing some sort of goodness-of-fit statistic.

Our method of calculating exposure ages uses production rate scaling factors for latitude and elevation initially described by Lal (1991) and later modified by Stone (2000) (henceforth, the Lal-Stone scaling scheme). We apply this scaling scheme to a set of calibration measurements (described below) to obtain reference production rates at sea level and high latitude as follows: for production by neutron spallation,  $4.87 \pm 0.33$  atoms  $\cdot$  g<sup>-1</sup>  $\cdot$  yr<sup>-1</sup> and  $29.8 \pm 1.6$  atoms  $\cdot$  g<sup>-1</sup>  $\cdot$  yr<sup>-1</sup> for <sup>10</sup>Be and <sup>26</sup>Al respectively, and for production by muons,  $0.11 \pm 0.01$  atoms  $\cdot$  g<sup>-1</sup>  $\cdot$  yr<sup>-1</sup> and  $0.8 \pm 0.04$  atoms  $\cdot$  g<sup>-1</sup>  $\cdot$  yr<sup>-1</sup>, yielding total reference production rates of  $4.98 \pm 0.34$  atoms  $\cdot$  g<sup>-1</sup>  $\cdot$  yr<sup>-1</sup> and  $30.6 \pm 1.7$  atoms  $\cdot$  g<sup>-1</sup>  $\cdot$  yr<sup>-1</sup>. These reference production rates fit the calibration data set with reduced  $\chi^2$  statistics of 0.97 and 0.3 for <sup>10</sup>Be and <sup>26</sup>Al respectively (see Appendix 2).

Our method of calculating exposure ages (described below) includes a major simplification of nuclide production by muons, in which production by muons and spallation are taken to have the same depth dependence. This is not important in exposure-age calculations, because sites that can be accurately exposure-dated are by definition those where surface erosion is slow, and therefore nuclide production by muons can be considered as equivalent to production by neutron spallation without loss of accuracy. When actually measuring erosion rates, on the other hand, it is important to take into account the fact that muons penetrate more deeply into rock than high-energy neutrons, and therefore much of the nuclide inventory at the surface is the result of production by muons at depth (as has been pointed out by, for example, Stone et al. (1998b) and Granger et al. (2001)). Thus it is important to use a description of nuclide production by muons which accurately depicts the production rate - depth profile. For erosion rate calculations, therefore, we replace the part of the Lal-Stone scaling scheme which deals with production by muons with the method of Heisinger et al. (2002b,a), which directly specifies production rates by muons as a function of site elevation and depth below the surface. For production by neutron spallation, we continue to use the Lal scaling factors, but we must apply the muon production rates calculated by Heisinger's method to the calibration data set to obtain compatible reference production rates for neutron spallation. Thus, we use slightly different reference production rates from neutron spallation in the erosion rate calculation. These are  $4.83 \pm 0.36$  atoms  $\cdot$  g<sup>-1</sup>  $\cdot$  yr<sup>-1</sup> (reduced  $\chi^2 = 1.0$ ) and  $29.5 \pm 1.9$  atoms  $\cdot$  g<sup>-1</sup>  $\cdot$  yr<sup>-1</sup> (reduced  $\chi^2 = 0.4$ ) for <sup>10</sup>Be and <sup>26</sup>Al respectively.

## 2.6 Production rate calibration data set

In calculating the reference production rates discussed above, we used a set of calibration measurements that is similar to that used by Stone (2000). This includes published measurements from Nishiizumi et al. (1989), Gosse and Klein (1996), Gosse et al. (1995), Stone et al. (1998a), Larsen (1996), Nishiizumi et al. (1996), Kubik et al. (1998), and Farber et al. (2005), as well as additional unpublished information provided by J. Gosse. This calibration data set is Appendix 2. In this work, we have done our best to incorporate recent improvements in the radiocarbon time scale (Reimer et al. (2004)) into relevant limiting radiocarbon ages for some of the calibration sites. Also, we have used a different averaging procedure than Stone (2000). In that work, each sample was equally weighted; here, as the number of samples in each calibration study differs widely, we have computed an error-weighted mean from all the samples at each calibration site, and then weighted each site equally in computing a summary average. These two points account for the small difference between the reference production rates derived here (e.g.,  $4.98 \text{ atoms} \cdot \text{g}^{-1} \cdot \text{yr}^{-1}$  for  $^{10}\text{Be}$ ) and in Stone (2000) ( $5.1 \text{ atoms} \cdot \text{g}^{-1} \cdot \text{yr}^{-1}$ ). Figures 2 and 3 show the calibration data set and the reference production rates derived therefrom. For the uncertainty in the reference production rates we take the standard deviation of the mean values from all the calibration sites.

## 2.7 Production rate correction factors

We take the surface production rate of nuclide  $i$  ( $\text{atoms} \cdot \text{g}^{-1} \cdot \text{yr}^{-1}$ ) at a sample site to be:

$$P_i = P_{i,ref} S_{i,geo} S_T S_{thick} \quad (1)$$

where  $P_{i,ref}$  is the reference production rate as described above and  $S_{geo}$  is the geographic scaling factor computed using either the Lal-Stone scaling scheme (for exposure-age calculations) or the Lal-Stone scaling scheme for production by spallation and the Heisinger description of production by muons (for erosion rate calculations), as described above. The thickness correction factor  $S_{thick}$  is only used in the exposure age calculation. It is based on nuclide production decreasing exponentially with depth with a single attenuation length  $\Lambda_{sp}$ . In the erosion rate calculations, sample thickness is accounted for in the integration of Equation 3 below. The correction factor for topographic shielding  $S_T$  is based on the assumption that the distribution of the cosmic-ray flux with zenith angle  $\theta$  is proportional to  $(\cos \theta)^{2.3}$ . Formulae for all of these correction factors appear in Appendix 1.

## 2.8 Exposure ages and erosion rates

The exposure age calculation uses the equation relating exposure age, erosion rate, and nuclide concentration from Lal (1991):

$$N_i = \frac{P_i}{\lambda_i + \frac{\epsilon}{\Lambda_{sp}}} \left( 1 - \exp \left[ - \left( \lambda_i + \frac{\epsilon}{\Lambda_{sp}} \right) t_{exp} \right] \right) \quad (2)$$

where  $N_i$  is the measured concentration of nuclide  $i$  (atoms  $\cdot$  g $^{-1}$ ),  $P_i$  is the total production rate of nuclide  $i$  in the sample (atoms  $\cdot$  g $^{-1}$   $\cdot$  yr $^{-1}$ ),  $\epsilon$  is the independently determined surface erosion rate (g  $\cdot$  cm $^{-2}$   $\cdot$  yr $^{-1}$ ), and  $t_{exp}$  is the exposure age (yr). This equation can be directly solved to yield  $t_{exp}$ .

The erosion rate calculation is based on the equation:

$$N_i = \int_0^\infty [P_{i,sp}(\epsilon t) + P_{i,\mu f}(\epsilon t) + P_{i,\mu-}(\epsilon t)] e^{-\lambda_i t} dt \quad (3)$$

where  $\epsilon$  is the erosion rate (here in g  $\cdot$  cm $^{-2}$   $\cdot$  yr $^{-1}$ ), and  $P_{i,sp}(z)$ ,  $P_{i,\mu f}(z)$ , and  $P_{i,\mu-}(z)$  are the production rates of nuclide  $i$  due to spallation, fast muon interactions, and negative muon capture, averaged over the sample thickness, as functions of depth. We take the depth dependence of production due to spallation to be exponential with attenuation length  $\Lambda_{sp}$ , and use the depth dependence of production by muons from Heisinger et al. (2002b,a). This equation cannot be solved directly for the erosion rate, so we use a numerical rootfinding algorithm.

Most erosion rates calculated from  $^{10}\text{Be}$  and  $^{26}\text{Al}$  measurements in the existing literature were calculated using the simple formulation of Lal (1991), that is, the limit of Equation 2 as  $t_{exp}$  goes to infinity:

$$N_i = \frac{P_i}{\lambda_i + \frac{\epsilon}{\Lambda_{sp}}} \quad (4)$$

This assumes that the depth dependence of the production rate is that of neutron spallation only, and disregards the fact that production by muons is attenuated less rapidly. As pointed out by Stone et al. (1998b) and Granger et al. (2001), given that the other assumptions of the method are satisfied, erosion rates calculated using Equation 4 underestimate the true erosion rate by at least a few percent in all cases, and by several tens of percent for low-elevation sites. Thus, the erosion rates calculated using the present method (Equation 3) will be systematically higher than many erosion rate measurements in the existing literature. Figure 4 gives an idea of the significance of this difference.

## 2.9 Error propagation

The challenge in providing a realistic uncertainty for calculated exposure ages and erosion rates is that there are few data available to establish the accuracy of many parts of the calculation. For example, we expect that the Lal-Stone scaling scheme is more accurate for certain locations and elevations than others, but no one has attempted to quantitatively estimate this. This means that the reported uncertainty in some parameters, for example, the reference nuclide production rates, also includes an unknown amount of uncertainty in some other parts of the calculation, for example, the geographic scaling scheme. Our goal here is to use a relatively straightforward method of error propagation that takes into account those uncertainties which we know about, while avoiding speculation about those uncertainties that we do not know very much about.

In the exposure-age calculation, we take account of uncertainty in the reference production rate (derived from the scatter in the calibration measurements as described above) and uncertainty in the measured nuclide concentrations (derived from the AMS measurement itself as well as the laboratory blank uncertainty). For the erosion-rate calculation, we add uncertainty in the nuclide production rate by muons (derived from the cross-section measurements in Heisinger et al. (2002b,a)). As the analytical standards to which our calibration measurements are normalized are associated with specific values of the  $^{10}\text{Be}$  and  $^{26}\text{Al}$  decay constants, we do not take account of uncertainty in the decay constants.

We report two separate uncertainties for each calculation. First, the ‘internal uncertainty’ takes only measurement uncertainty in the nuclide concentration into account. This is useful in situations where one wishes to compare exposure ages or erosion rates derived from  $^{26}\text{Al}$  and  $^{10}\text{Be}$  measurements on samples from a single study area. For example, one common such situation arises when asking whether exposure ages of adjacent boulders on a single moraine agree or disagree. One should use the internal uncertainty to answer this question. Second, the ‘external uncertainty’ also accounts for uncertainties in the nuclide production rate. One should use the external uncertainty when comparing exposure ages from widely separated locations, or for comparing exposure ages to ages generated by other techniques, for example, radiocarbon dating, varve counting, or ice-core stratigraphy.

We actually calculate the uncertainties by assuming that the uncertainties in the input parameters are normal and independent, and that the result is linear with respect to all of the uncertain parameters, and adding in quadrature in the usual fashion (e.g., Bevington and Robinson, 1992). This method has several disadvantages, the major one being that it does not capture the fact that the actual uncertainties in

our results are not symmetrical around the central value. The fact that we cannot incorporate non-ideal probability distributions for the input parameters is a secondary disadvantage, although it is mitigated by the fact that there is little evidence to suggest whether or not the uncertainty in these input parameters is in fact asymmetric or otherwise unusual. In principle we could avoid both of these difficulties by using a Monte Carlo method of error propagation. We have chosen not to do so here for three reasons: First, at present there are relatively few input parameters with known uncertainties. Second, we are not aware at present of any complicated uncertainty distributions for the input parameters that require special treatment. Finally, keeping this issue in perspective relative to actual geological applications of cosmogenic-nuclide measurements, we are not aware of any studies where the difference between asymmetrical and symmetrical uncertainties would at all affect the conclusions of the study.

### **3 Likely areas of future improvement.**

Most of the significant inconsistencies and simplifications that we have called attention to are the subject of active research, primarily as part of the CRONUS-Earth project, and will presumably be the focus of future improvements. The following parts of our method are likely to be significantly improved in future:

*Scaling schemes that take account of paleomagnetic variation.* Several such scaling methods exist in the literature at present; the difficulty in applying them is the fact that the spatial and temporal distribution of the existing geological calibration data set is poorly suited to testing them. Additional geological calibration measurements will very likely improve this situation in future.

*Topographic and geometric shielding effects.* The topographic and geometric shielding corrections in our method are highly simplified. While adequate for sites with simple geometries, they limit users' ability to study processes that take place at severely shielded locations or within oddly shaped landforms. Physical models of particle transport, geological calibration measurements at severely shielded sites, and a better effort to incorporate the angular and energy distribution of incoming cosmic-ray particles, will all provide better means of carrying out this part of the calculation.

*Treatment of fast muons.* The key uncertainty in the treatment of fast muon interactions is the energy dependence of the reaction cross-sections. Our understanding of this uncertainty will likely be much improved in future by new measurements of nuclide concentrations in subsurface samples.

*Uncertainties.* The main difficulty in assigning uncertainties to exposure ages and erosion rates is that the spatial and temporal distribution of the uncertainty in the

geographic scaling factors is unknown. Again, present and future efforts to better understand the physical basis of production rate scaling schemes, as well as a larger calibration data set, will result in a more realistic understanding of the accuracy of exposure dating relative to other dating methods.

#### 4 Acknowledgements

This work is part of the CRONUS-Earth project, and is supported by NSF grant EAR-0345574. It is CRONUS-Earth Contribution No. 1. Kuni Nishiizumi, Dan Farber, Lewis Owen, and Bill Phillips provided valuable help in reviewing and testing the MATLAB code and the user interface.

#### References

- Bevington, P., Robinson, D., 1992. Data Reduction and Error Analysis for the Physical Sciences. WCB McGraw-Hill.
- Bierman, P., Nichols, K., 2004. Rock to sediment – slope to sea with  $^{10}\text{Be}$  – rates of landscape change. Annual Reviews of Earth and Planetary Sciences 32, 215–255.
- Bierman, P., Steig, E., 1996. Estimating rates of denudation using cosmogenic isotope abundances in sediment. Earth Surface Processes and Landforms 21, 125–139.
- Brown, E., Stallard, R., Larsen, M., G.M., R., Yiou, F., 1995. Denudation rates determined from the accumulation of in-situ-produced  $^{10}\text{Be}$  in the Luquillo Experimental Forest, Puerto Rico. Earth and Planetary Science Letters 129, 193–202.
- Desilets, D., Zreda, M., 2003. Spatial and temporal distribution of secondary cosmic-ray nucleon intensities and applications to in-situ cosmogenic dating. Earth and Planetary Science Letters 206, 21–42.
- Dunai, T., 2001. Influence of secular variation of the magnetic field on production rates of in situ produced cosmogenic nuclides. Earth and Planetary Science Letters 193, 197–212.
- Dunne, J., Elmore, D., Muzikar, P., 1999. Scaling factors for the rates of production of cosmogenic nuclides for geometric shielding and attenuation at depth on sloped surfaces. Geomorphology 27, 3–12.
- Farber, D., Hancock, G., Finkel, R., Rodbell, D., 2005. The age and extent of tropical alpine glaciation in the Cordillera Blanca, Peru. Journal of Quaternary Science 20, 759–776.
- Gosse, J., Klein, J., 1996. Production rate of *in-situ* cosmogenic  $^{10}\text{Be}$  in quartz at high altitude and mid latitude. Radiocarbon 38, 154–155.
- Gosse, J. C., Evenson, E., Klein, J., Lawn, B., Middleton, R., 1995. Precise cos-

- mogenic  $^{10}\text{Be}$  measurements in western North America: support for a global Younger Dryas cooling event. *Geology* 23, 877–880.
- Gosse, J. C., Phillips, F. M., 2001. Terrestrial in situ cosmogenic nuclides: theory and application. *Quaternary Science Reviews* 20, 1475–1560.
- Granger, D., Riebe, C., Kirchner, J., Finkel, R., 2001. Modulation of erosion on steep granitic slopes by boulder armoring, as revealed by cosmogenic  $^{26}\text{Al}$  and  $^{10}\text{Be}$ . *Earth and Planetary Science Letters* 186, 269–281.
- Granger, D. E., Kirchner, J., Finkel, R., 1996. Spatially averaged long-term erosion rates measured from in situ-produced cosmogenic nuclides in alluvial sediment. *Journal of Geology* 104, 249–257.
- Heisinger, B., Lal, D., Jull, A. J. T., Kubik, P., Ivy-Ochs, S., Knie, K., Nolte, E., 2002a. Production of selected cosmogenic radionuclides by muons: 2. Capture of negative muons. *Earth and Planetary Science Letters* 200 (3-4), 357–369.
- Heisinger, B., Lal, D., Jull, A. J. T., Kubik, P., Ivy-Ochs, S., Neumaier, S., Knie, K., Lazarev, V., Nolte, E., 2002b. Production of selected cosmogenic radionuclides by muons 1. Fast muons. *Earth and Planetary Science Letters* 200 (3-4), 345–355.
- Kubik, P., Ivy-Ochs, S., Masarik, J., Frank, M., Schluchter, C., 1998.  $^{10}\text{Be}$  and  $^{26}\text{Al}$  production rates deduced from an instantaneous event within the dendro-calibration curve, the landslide of köfels, Ötz Valley, Austria. *Earth and Planetary Science Letters* 161, 231–241.
- Lal, D., 1991. Cosmic ray labeling of erosion surfaces: in situ nuclide production rates and erosion models. *Earth Planet. Sci. Lett.* 104, 424–439.
- Lal, D., Chen, J., 2005. Cosmic ray labeling of erosion surfaces ii: Special cases of exposure histories of boulders, soil, and beach terraces. *Earth and Planetary Science Letters* 236, 797–813.
- Larsen, P., 1996. In-situ production rates of cosmogenic  $^{10}\text{Be}$  and  $^{26}\text{Al}$  over the past 21,500 years determined from the terminal moraine of the Laurentide Ice Sheet, north-central New Jersey. Ph.D. thesis, University of Vermont.
- Masarik, J., Frank, M., Schäfer, J., Wieler, R., 2001. Correction of in situ cosmogenic nuclide production rates for geomagnetic field intensity variations during the past 800,000 years. *Geochimica Et Cosmochimica Acta* 65, 2995–3003.
- Masarik, J., Wieler, R., 2003. Production rates of cosmogenic nuclides in boulders. *Earth and Planetary Science Letters* 216, 201–208.
- Nishiizumi, K., 2002.  $^{10}\text{Be}$ ,  $^{26}\text{Al}$ ,  $^{36}\text{Cl}$ , and  $^{41}\text{Ca}$  ams standards: Abstract o16-1. In: 9th Conference on Accelerator Mass Spectrometry. p. 130.
- Nishiizumi, K., 2004. Preparation of  $^{26}\text{Al}$  AMS standards. *Nuclear Instruments and Methods in Physics Research B* 223-224, 388–392.
- Nishiizumi, K., Finkel, R., Klein, J., Kohl, C., 1996. Cosmogenic production of  $^7\text{Be}$  and  $^{10}\text{Be}$  in water targets. *Journal of Geophysical Research* 101 (B10), 22,225–22,232.
- Nishiizumi, K., Winterer, E., Kohl, C., Klein, J., Middleton, R., Lal, D., Arnold, J., 1989. Cosmic ray production rates of  $^{26}\text{Al}$  and  $^{10}\text{Be}$  in quartz from glacially polished rocks. *J. Geophys. Res.* 94, 17,907–17,915.
- Pigati, J. S., Lifton, N., 2004. Geomagnetic effects on time-integrated cosmogenic

- nuclide production with emphasis on in situ  $^{14}\text{C}$  and  $^{10}\text{Be}$ . *Earth and Planetary Science Letters* 226, 193–205.
- Reimer, P., Baillie, M., Bard, E., Bayliss, A., Beck, J., Bertrand, C., Blackwell, P., Buck, C., Burr, G., Cutler, K., Damon, P., Edwards, R., Fairbanks, R., Friedrich, M., Guilderson, T., Hogg, A., Hughen, K., Kromer, B., McCormac, G., Manning, S., Ramsey, C., Reimer, R., Remmele, S., Southon, J., Stuiver, M., Talamo, S., Taylor, F., van der Plicht, J., Weyhenmeyer, C., 2004. INTCAL04 terrestrial radiocarbon age calibration, 0-26 cal kyr bp. *Radiocarbon* 46, 1029–1058.
- Stone, J., Ballantyne, C., Fifield, L., 1998a. Exposure dating and validation of periglacial weathering limits, northwest Scotland. *Geology* 26, 587–590.
- Stone, J. O., 2000. Air pressure and cosmogenic isotope production. *Journal of Geophysical Research* 105 (B10), 23753–23759.
- Stone, J. O. H., Evans, J. M., Fifield, L. K., Allan, G. L., Cresswell, R. G., 1998b. Cosmogenic chlorine-36 production in calcite by muons. *Geochimica Et Cosmochimica Acta* 62 (3), 433–454.
- von Blanckenburg, F., 2006. The control mechanisms of erosion and weathering at basin scale from cosmogenic nuclides in river sediment. *Earth and Planetary Science Letters* 242, 224–239.

Table 1  
 Input data needed to calculate a  $^{10}\text{Be}$  or  $^{26}\text{Al}$  exposure age or erosion rate

Field	Units	Comments
Sample name	Text	
Latitude	Decimal degrees	South latitudes are negative.
Longitude	Decimal degrees	West longitudes are negative.
Elevation (atmospheric pressure)	m (hPa)	Sample elevation can be specified as either meters above sea level or as mean atmospheric pressure at the site. If elevation is given, one must also select an atmosphere approximation to use for calculating the atmospheric pressure. Two are available: the ICAO standard atmosphere and one designed for Antarctica (see Stone (2000) for discussion).
Sample thickness	cm	
Sample density	$\text{g} \cdot \text{cm}^{-3}$	
Shielding correction	nondimensional, between 0 and 1	Ratio of the production rate at the obstructed site to the production rate at a site at the same location and elevation, but with a flat surface and a clear horizon.
Erosion rate	$\text{cm} \cdot \text{yr}^{-1}$	The erosion rate of the sample surface inferred from independent evidence, to be taken into account when computing the exposure age. Only required for exposure-age calculations.
Nuclide concentrations	$\text{atoms} \cdot \text{g}^{-1}$	$^{10}\text{Be}$ and $^{26}\text{Al}$ concentrations in quartz in the sample. Should be normalized to the Nishiizumi $^{26}\text{Al}$ and $^{10}\text{Be}$ standards. Should account for laboratory process and carrier blanks.
Uncertainties in nuclide concentrations	$\text{atoms} \cdot \text{g}^{-1}$	1-standard error analytical uncertainties in the measured nuclide concentrations. Should account for all sources of analytical error, including AMS measurement uncertainty, Al or Be concentration measurement uncertainty, and blank uncertainty.

Table 2  
Results of an exposure age calculation

Field	Units	Comments
Exposure age	yr	
Internal uncertainty	yr	Takes analytical uncertainties into account only.
External uncertainty	yr	Takes production rate and decay constant uncertainties into account as well.
Thickness scaling factor	nondimensional	Ratio of production rate in the sample to production rate at the surface.
Shielding correction	nondimensional	Re-reports the submitted value.
Geographic scaling factor	nondimensional	According to Stone (2000).
Local production rate due to spallation	$\text{atoms} \cdot \text{g}^{-1} \cdot \text{yr}^{-1}$	Thickness-averaged. Includes shielding correction.
Local production rate due to muons	$\text{atoms} \cdot \text{g}^{-1} \cdot \text{yr}^{-1}$	Thickness-averaged. Includes shielding correction.
Total local production rate	$\text{atoms} \cdot \text{g}^{-1} \cdot \text{yr}^{-1}$	Thickness-averaged. Includes shielding correction.

Table 3  
Results of an erosion rate calculation

Field	Units	Comments
Erosion rate	$\text{g} \cdot \text{cm}^{-2} \cdot \text{yr}^{-1}$	
Erosion rate	$\text{m} \cdot \text{Myr}^{-1}$	
Internal uncertainty	$\text{m} \cdot \text{Myr}^{-1}$	Takes analytical uncertainties into account only.
External uncertainty	$\text{m} \cdot \text{Myr}^{-1}$	Takes production rate and decay constant uncertainties into account as well.
Local production rate due to spallation	$\text{atoms} \cdot \text{g}^{-1} \cdot \text{yr}^{-1}$	Thickness-averaged. Includes shielding correction.
Local production rate due to fast muon interactions	$\text{atoms} \cdot \text{g}^{-1} \cdot \text{yr}^{-1}$	Thickness-averaged.
Local production rate due to negative muon capture	$\text{atoms} \cdot \text{g}^{-1} \cdot \text{yr}^{-1}$	Thickness-averaged.
Total local production rate	$\text{atoms} \cdot \text{g}^{-1} \cdot \text{yr}^{-1}$	Sum of the above three components.

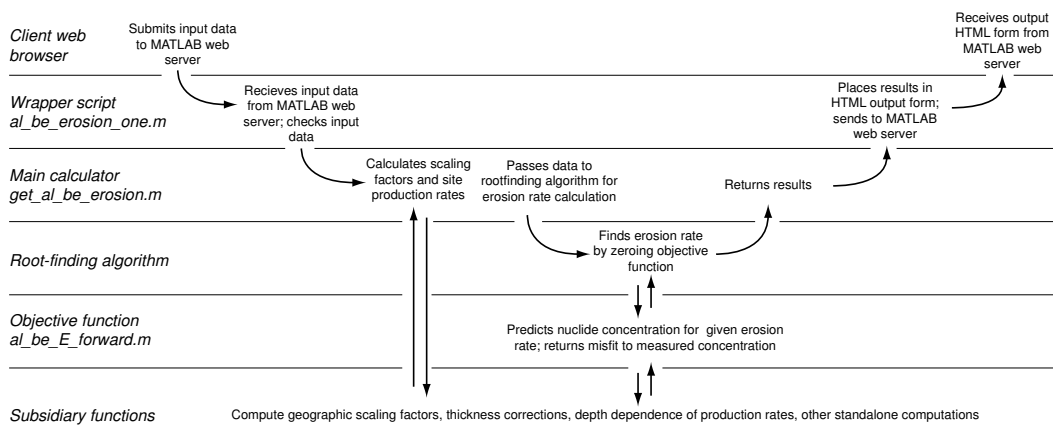


Fig. 1. Flow of information between HTML input and output forms, the MATLAB web server, and MATLAB functions that carry out calculations. This example shows the HTML and MATLAB code involved in an erosion rate calculation; exposure age calculations are similar.

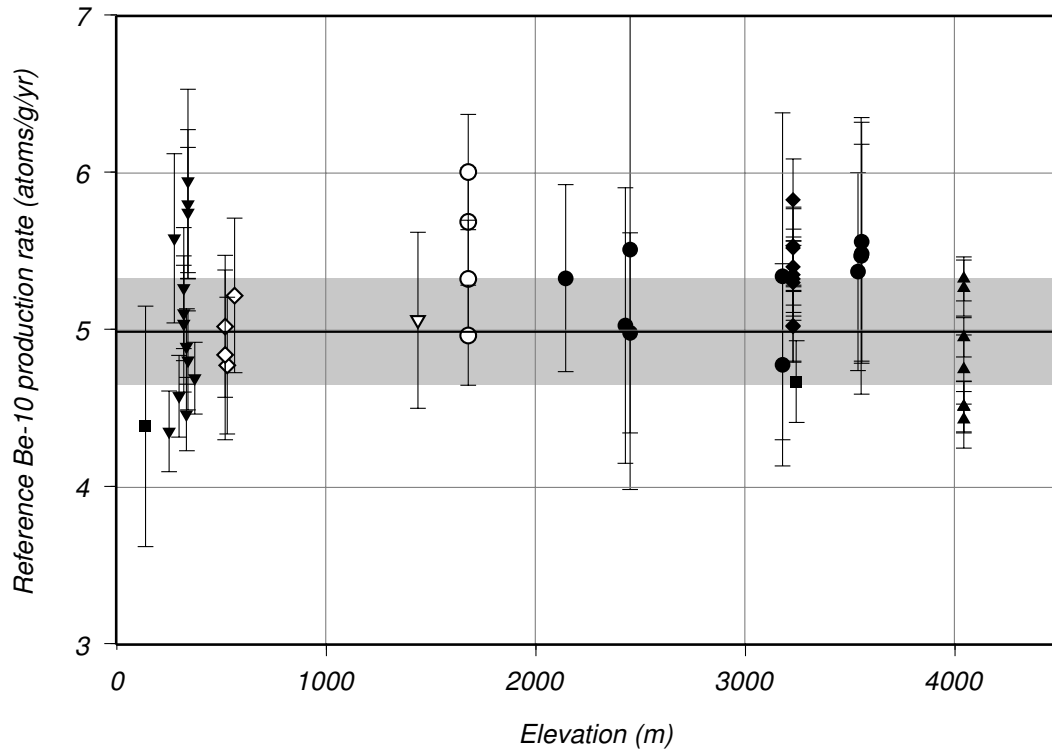


Fig. 2. Reference  $^{10}\text{Be}$  production rates at sea level and high latitude inferred from geological calibration sites, using the scaling scheme of Stone (2000). Symbols are as follows: filled circles, Sierra Nevada (Nishiizumi et al., 1989); open circles, Köfels landslide, Austria (Kubik et al., 1998); filled diamonds, Titcomb Basin, Wyoming (Gosse et al., 1995; Gosse and Klein, 1996, Gosse, unpublished data); open diamonds, Scotland (Stone et al., 1998a); filled downward-pointing triangles, New Jersey (Larsen, 1996); open downward-pointing triangles, Lake Bonneville, Utah (Gosse and Klein, 1996); filled upward-pointing triangles, Breque, Peru (Farber et al., 2005); open squares, water-target experiments (Nishiizumi et al., 1996). Error bars show  $1\text{-}\sigma$  uncertainties. The dashed line and grey band show the summary reference production rate and  $1\text{-}\sigma$  uncertainty of  $4.98 \pm 0.34$  atoms  $\cdot$  g $^{-1}$   $\cdot$  yr $^{-1}$  inferred from the data.

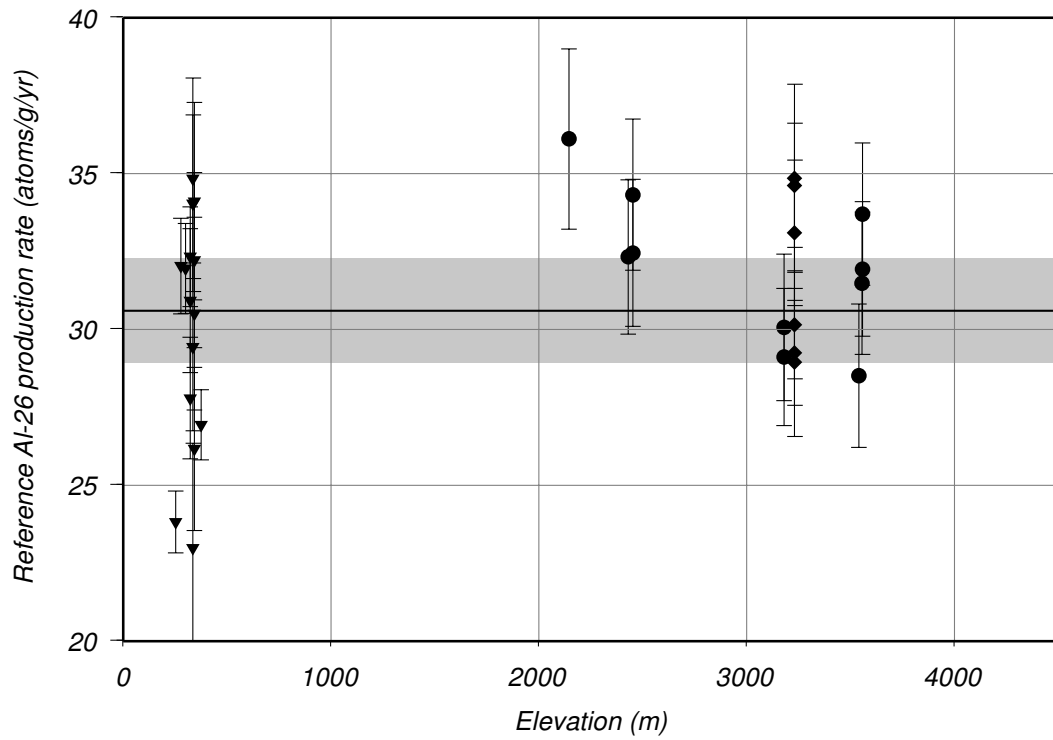


Fig. 3. Reference  $^{26}\text{Al}$  production rates at sea level and high latitude inferred from geological calibration sites, using the scaling scheme of Stone (2000). The symbols are the same as in Figure 2.

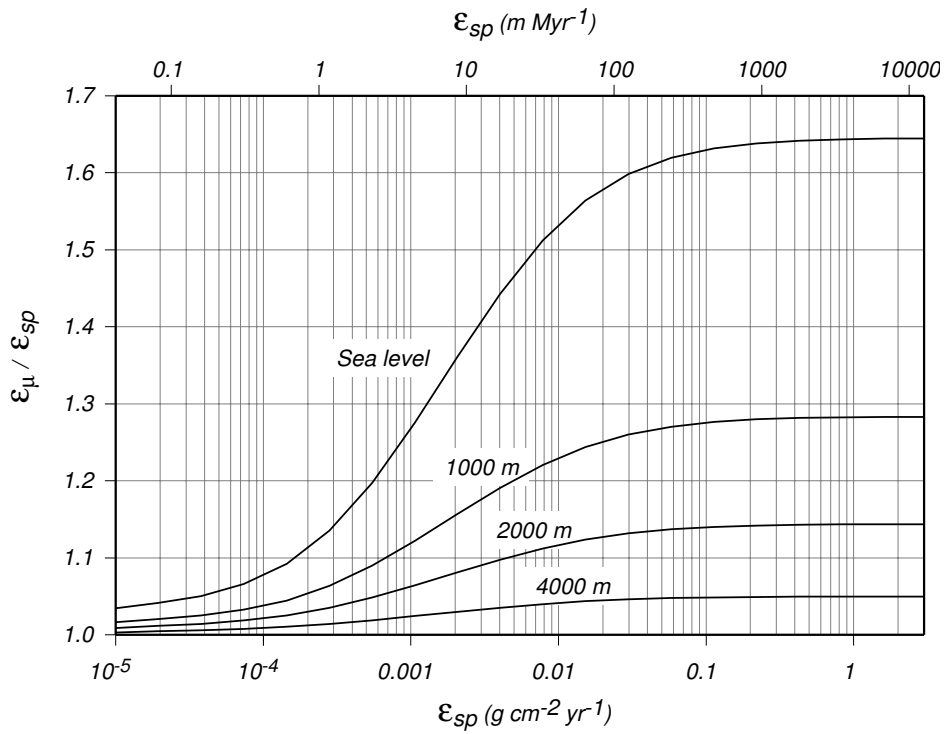


Fig. 4. Difference between calculated erosion rates that take account of subsurface nuclide production by muons ( $\epsilon_{\mu}$ ; Equation 3) and those that do not ( $\epsilon_{sp}$ ; Equation 4). The two different x-axis scales are related by a material density of  $2.65 \text{ g} \cdot \text{cm}^{-3}$ .